IAC–2016–C1.7.1.x35369

De-Orbiting and Re-entry Analysis with Generalised Intrusive Polynomial Expansions

Carlos Ortega Absil
University of Strathclyde, United Kingdom, carlos.ortega@strath.ac.uk

Romain Serra
University of Strathclyde, United Kingdom, romain.serra@strath.ac.uk

Annalisa Riccardi
University of Strathclyde, United Kingdom, annalisa.riccardi@strath.ac.uk

Massimiliano Vasile
University of Strathclyde, United Kingdom, massimiliano.vasile@strath.ac.uk

Generalised Intrusive Polynomial Expansion (GIPE) is a novel method for the propagation of multidimensional compact sets through dynamical systems. It generalises the more widely-known Taylor Differential Algebra in that it allows the use of generic polynomial representations of a multi-dimensional set. In particular the paper proposes the use of truncated Tchebycheff series. Unlike Taylor expansions, that are not generally convergent, Tchebycheff expansions provide fast uniform convergence with relaxed continuity and smoothness requirements, guaranteeing near-minimax approximation. This methodology has proven to be competitive for uncertainty propagation in orbital dynamics, especially when dealing with a large number of uncertain variables. Moreover, it provides the user with a complete polynomial representation of the uncertain region at any point of the propagation, allowing for remarkable gain of insight into the underlying properties of the uncertain dynamics. The paper presents the application of the GIPE approach to the end-of-life analysis of Low Earth Orbit satellites, with special emphasis on the case of the de-orbiting and re-entry of GOCE and the de-orbiting of objects with high area to mass ratio. The effect of various sources of uncertainty on the end-of-life dynamics is thus analysed, such as the drag model or the accuracy of the initial orbit determination.

I. Introduction

The paper will consider two different studies. The first one is the end-of-life trajectory of GOCE. The ESA vehicle, which re-entered the atmosphere in November 2013, was intensively tracked during its final days. This case is studied by means of a high-fidelity 3-dof propagator in a geocentric cartesian reference frame. The second example concerns objects with high area-to-mass ratio, such as pieces of a solar panel. For instance, it could model a cloud of fragments resulting from a collision in Low Earth Orbit (LEO). This case is tackled by means of simplified dynamics in the osculating orbital elements and refined with the aid of the aforementioned propagator. Both these cases will demonstrate low initial altitudes, leading to re-entry in a matter of days as drag strongly impacts the orbital motion. For this application, GIPE represents a valuable approach to simulate a range of values for various uncertain quantities, such as initial orbit and atmospheric conditions. Being capable of propagating the uncertain set through the dynamics at once, a complete representation of the uncertain quantities of interest is available to the user at any point of the simulation, making dynamic analysis possible. A comparison is provided between Taylor Differential Algebra and a GIPE approach based on Tchebycheff approximation, where their numerical stability properties for LEO dynamics are put to the test.

Taylor Differential Algebra is based on the Truncated Power Series Algebra (TPSA) introduced by Berz in 1986[1,2] and is nowadays a popular methodology in the space sector. Recent applications in astrodynamics and celestial mechanics can be found in the work of Di Lizia et al.[3] and Armellin et al.[4],[5] and in the work of Jorba et al.[6]

Brisebarre and Joldes[7] provided in 2010 a formal comparison of the TPSA with Taylor, Tchebycheff and Newton basis in the univariate case, proving that enhanced accuracy can be obtained by means of hyperinterpolation-based approaches with respect to derivative-based algebras. In the case of Tchebycheff basis, the development of a multi-variate algebra and its application in astrodynamics, to the knowledge of the authors, appears in 2015 with the work of Riccardi et al.[8]

An important feature of this study is that it will test the hypothesis that hyperinterpolation-based approaches are more stable when using piece-wise-defined models that do not provide infinite differentiability between their sub-domains. All results presented hereby make use of the implementation of GIPE provided in SMART-UQ.[9]

II. Intrusive approach

Given a continuous, piece-wise differentiable, function $f(\mathbf{x}) : \Omega \subset \mathbb{R}^d \to \mathbb{R}$, we consider the approximation

$$f(\mathbf{x}) = P(\mathbf{x}) + r(\varepsilon) = \sum_{\mathbf{i},|\mathbf{i}|\leq n} p_{\mathbf{i}}\alpha_{\mathbf{i}}(\mathbf{x}) + r(\varepsilon)\,, \qquad [1]$$

where $\Omega = [-1,1]^d$, $\mathbf{x} \in \Omega$, $\mathbf{i} \in [0,n]^d \subset \mathbb{N}^d$, $|\mathbf{i}| = \sum_{r=1}^{d} i_r$, $r(\varepsilon)$ is a remainder (with $\varepsilon \in \Omega$), and $\alpha_{\mathbf{i}}(\mathbf{x})$ is a polynomial basis of choice, up to order n. The number of coefficients for a complete expansion is given by

$$\mathcal{N}_{d,n} = \binom{n+d}{d} = \frac{(n+d)!}{n!\,d!}\,, \qquad [2]$$

The polynomial $P(\mathbf{x})$ belongs to the function space $\mathcal{P}_{n,d}(\alpha_i)$ of polynomials of order n in d dimensions, in the α_i basis.

The definition of the polynomials can be extended to a generic hyper-rectangle $\overline{\Omega} = [\mathbf{a},\mathbf{b}] \subseteq \mathbb{R}^d$; being $\tau : \overline{\Omega} \to \Omega$ the linear mapping between the two regions, the generalised expansions are defined over $\overline{\Omega}$ by

$$\alpha_{\mathbf{i}}(\mathbf{x}) = \alpha_{\mathbf{i}}(\tau(\mathbf{x}'))\,, \qquad [3]$$

where $\mathbf{x}' \in \overline{\Omega}$. So without loss of generality the domain Ω is considered hereafter.

II.i Polynomial Algebra

The function space $\mathcal{P}_{n,d}(\alpha_i)$ can be equipped with a set of elementary arithmetic operations, generating an algebra on the space of polynomials or polynomial space in the α_i basis, such that, given two elements $A(\mathbf{x})$, $B(\mathbf{x})$ approximating any two functions $f_A(\mathbf{x})$ and $f_B(\mathbf{x})$,

$$f_A(\mathbf{x}) \oplus f_B(\mathbf{x}) \sim A(\mathbf{x}) \otimes B(\mathbf{x})\,, \qquad [4]$$

where $\oplus \in \{+,-,\cdot,/\}$ and $\otimes$ is the corresponding operation in $\mathcal{P}_{n,d}(\alpha_i)$. This allows one to define the algebra $(\mathcal{P}_{n,d}(\alpha_i),\otimes)$, of dimension $\dim(\mathcal{P}_{n,d}(\alpha_i),\otimes) = \mathcal{N}_{d,n}$, the elements of which belong to the polynomial ring in d indeterminates $\mathbb{R}[\mathbf{x}]$ and have degree up to n. Each element $P(\mathbf{x})$ of the algebra, is uniquely identified by the set of its coefficients $\mathbf{p} = \{p_{\mathbf{i}} : |\mathbf{i}| \leq n\} \in \mathbb{R}^{\mathcal{N}_{d,n}}$ such that

$$P(\mathbf{x}) = \sum_{\mathbf{i},|\mathbf{i}|\leq n} p_{\mathbf{i}}\alpha_{\mathbf{i}}(\mathbf{x})\,. \qquad [5]$$

The operations of addition and subtracting are defined as follows: being $A(\mathbf{x})$ and $B(\mathbf{x})$ two elements of $(\mathcal{P}_{n,d}(\alpha_i),\otimes)$, identified by the set of coefficients $\mathbf{a},\mathbf{b} \in \mathbb{R}^{\mathcal{N}_{d,n}}$, respectively, the result of their sum or difference is

$$C(\mathbf{x}) = A(\mathbf{x}) \pm B(\mathbf{x})\,, \qquad [6]$$

identified by the set of coefficients $\mathbf{c} \in \mathbb{R}^{\mathcal{N}_{d,n}}$ such that

$$\mathbf{c} = \mathbf{a} \pm \mathbf{b}\,. \qquad [7]$$

The product of two polynomials is defined accordingly to the basis used. For example, the product between two monomial basis is defined as

$$\mathbf{x}^{\mathbf{i}} \cdot \mathbf{x}^{\mathbf{j}} = \begin{cases} \mathbf{x}^{\mathbf{i}+\mathbf{j}} & \text{if } |\mathbf{i}+\mathbf{j}| \leq \text{n} \\ 0 & \text{otherwise} \end{cases}\,, \qquad [8]$$

the result thus truncated to the order n. Given that the computational cost of multiplying two polynomials not in the monomial basis is generally higher, arithmetic operations can always be performed in the monomial basis, as far as the transformation

$$\nu \,:\, \mathcal{P}_{n,d}(\alpha_i) \longrightarrow \mathcal{P}_{n,d}(\phi_i) \qquad [9]$$

from the current basis into the monomial basis ϕ_i can be defined. One can now take two general polynomial expansions $A(\mathbf{x})$ and $B(\mathbf{x})$, express them in terms of monomials, and apply the following multiplication operation

$$\nu(A(\mathbf{x})) \cdot \nu(B(\mathbf{x})) = \left(\sum_{\mathbf{i},|\mathbf{i}|\leq n} a_{\mathbf{i}}\mathbf{x}^{\mathbf{i}}\right)\left(\sum_{\mathbf{i},|\mathbf{i}|\leq n} b_{\mathbf{i}}\mathbf{x}^{\mathbf{i}}\right)\,. \qquad [10]$$

By collecting all the contributions to each monomial $\mathbf{x}^{\mathbf{i}}$, it is possible to compute the coefficients of the product approximation with substantially less operations than for the case of multiplication in the polynomial ring $\mathbb{R}[\mathbf{x}]$.

In the same way as for arithmetic operations, it is possible to define a composition rule in the polynomial algebra such that

$$g(\mathbf{y}(\mathbf{x})) \sim G(\mathbf{y}) \circ \mathbf{Y}(\mathbf{x})\,, \qquad [11]$$

where $\circ$ is the composition function on $(\mathcal{P}_{n,d}(\alpha_i),\otimes)$ and $g(\mathbf{x})$ and $\mathbf{y}(\mathbf{x})$ are, respectively, a multivariate function and an array of d multivariate functions in the real space, with $G(\mathbf{x})$ and $\mathbf{Y}(\mathbf{x})$ their polynomial expansions. The composition rule can be used to introduce the counterpart, in the algebra, of division operation and elementary function: being $h(y)$ any of the functions $\{1/y, \sin(y), \cos(y), \exp(y), \log(y), ...\}$, $H(y)$ its univariate polynomial expansion, $f(\mathbf{x})$ a multivariate function and $F(\mathbf{x})$ its multivariate polynomial expansion, their composition is approximated by

$$h(f(\mathbf{x})) \sim H(y) \circ F(\mathbf{x})\,, \qquad [12]$$

in which $\circ$ denotes the composition of an element of the algebra with an univariate polynomial

$$\circ \,:\, \mathcal{P}_{n,1}(\alpha_i) \times \mathcal{P}_{n,d}(\alpha_i) \longrightarrow \mathcal{P}_{n,d}(\alpha_i)\,. \qquad [13]$$

Being composition defined between polynomials in the same basis, to perform multiplication between polynomials in the monomial basis and avoid the computational cost of transforming the result back to the current basis, composition between polynomials in the monomial basis can only be used. In this case, being $H(x)$ the expansion of an elementary function in the chosen polynomial basis, it is

$$h(f(\mathbf{x})) \sim \nu(H(x)) \circ F_\phi(\mathbf{x})\,, \qquad [14]$$

where $F_\phi(\mathbf{x})$ is the approximation in the monomial basis of $f(\mathbf{x})$. Hence, without loss of generality, all arithmetic operations can be performed in $\mathcal{P}_{n,d}(\phi_i)$.

It needs to be noted that for the case of Tchebycheff expansions, given that high order terms have contribution to low order terms in the monomial basis*, $H(x)$ is expanded up to no less than 1.5 times the order of the algebra and $\nu(H(x))$ is truncated afterwards. This has been found to minimise the loss of accuracy when the change of basis is performed. Hence, for the proposed Tchebycheff approximation the transformation ν is between the functional spaces

$$\nu \,:\, \mathcal{P}_{\lceil 1.5n \rceil,d}(\alpha_i) \longrightarrow \mathcal{P}_{n,d}(\phi_i)\,, \qquad [15]$$

where α_i is the Tchebycheff basis and ϕ_i the monomial basis.

Note that since $H(x)$ is an univariate polynomial, the change-of-basis matrix is of order $n+1$, or size $(n+1) \times (\lceil 1.5n \rceil + 1)$ in case of Tchebycheff approximation, instead of order $\mathcal{N}_{d,n}$, rendering the conversion computationally cheaper than in the multivariate case.

II.ii Set Propagation in Dynamical Systems

Consider the following Cauchy problem

$$\begin{cases} \dot{\mathbf{x}} & = f(\mathbf{x}, \mathbf{b}) \\ \mathbf{x}(t_0) & = \mathbf{x_0} \end{cases}\,, \qquad [16]$$

where $\mathbf{b} \in \Upsilon \subseteq \mathbb{R}^q$ is a vector of model parameters and the initial conditions have value $\mathbf{x_0} \in \Sigma_0 \subseteq \mathbb{R}^c$ so that $d = q + c$. We can now propagate the set $\Omega = \Upsilon \times \Sigma_0$ through the dynamics (16) by representing $\mathbf{x}_0$ and $\mathbf{b}$ as elements of the algebra $(\mathcal{P}_{n,d}(\alpha_i), \otimes)$ and applying any integration scheme with operations defined in the algebra.

* If we consider for example the forth order term of the univariate basis $C_4(x) = 8x^4 - 8x^2 + 1$, this has a contribution to the second order term of the monomial basis.

As an example, if $\mathbf{X}_0 := (X_1(\mathbf{x}), ..., X_c(\mathbf{x}))$ and $\mathbf{B} := (B_1(\mathbf{x}), .., B_q(\mathbf{x}))$ are initialised as elements of the algebra:

$$\begin{aligned} X_1(\mathbf{x}) &= \alpha_{\mathbf{1}_1}(\mathbf{x})\,, & B_1(\mathbf{x}) &= \alpha_{\mathbf{1}_{c+1}}(\mathbf{x})\,, \\ X_2(\mathbf{x}) &= \alpha_{\mathbf{1}_2}(\mathbf{x})\,, & B_2(\mathbf{x}) &= \alpha_{\mathbf{1}_{c+2}}(\mathbf{x})\,, \\ &\dots & &\dots \\ X_c(\mathbf{x}) &= \alpha_{\mathbf{1}_c}(\mathbf{x})\,, & B_q(\mathbf{x}) &= \alpha_{\mathbf{1}_d}(\mathbf{x})\,, \end{aligned} \qquad [17]$$

where $\alpha_{\mathbf{1}_j}(\mathbf{x})$ is the first order base in the j-th component. If a simple Euler scheme is used, then at each integration step one has:

$$\mathbf{X}_k = \mathbf{X}_{k-1} + \Delta t\ \mathbf{F}_{k-1}, \qquad [18]$$

where $\mathbf{F}_0$ is the polynomial approximation of $f(\mathbf{x}_0, \mathbf{b})$, obtained evaluating in the algebra the right-hand side in $\mathbf{X}_0$ and $\mathbf{B}$. Hence $\mathbf{X}_k$ is the polynomial representation of the system flow at the k^{th} time-step.

III. Re-entry dynamics

Two different ways to perform orbit propagation have been interfaced with the aforementioned intrusive approach, namely with Cartesian and Keplerian coordinates. In this work, the former is more elaborate than the latter in the sense that is takes into account orbital perturbations in a more precise way. Both are described in this section.

III.i Propagation with Cartesian coordinates

This propagator is a C++ implementation of Montenbruck and Gill[10] for a spherical spacecraft. The state vector consists of the Cartesian coordinates for position and velocity in an inertial frame. Due to the low altitudes considered in this study, only two forces are included in the dynamics: Earth's gravity (up to order and degree 9 in the geopotential) and atmospheric drag. In particular, the latter is based on the Jacchia-Gill representation of density. In this model, a standard value for the logarithm of density is computed from bi-variate polynomials (functions of altitude and exospheric temperature), before adding various contributions such as seasonal or latitudinal corrections. These polynomials being piece-wise defined on 2-D sub-intervals, they can be handled for pointwise propagation via 'if' conditions. However, it is not as simple for the algebra, especially for the Tchebycheff approach. For Taylor expansion, it is enough to use the central point as the reference to know in what sub-interval the model needs to be locally approximated. On the other hand, Tchebycheff interpolation considers a whole interval that can lie in between two sub-intervals. The solution chosen here is twofold. Since there are only two ranges for temperature, the transition between the two is generally represented with a sigmoid function i.e. the different

possibilities are both interpolated and the final result is a weighted sum of the two. As for altitude, on the other hand, when the range of the polynomial is expected to overlap two sub-intervals, the density function is still approximated with Tchebycheff polynomials, but it is done via bivariate approximation of the piece-wise defined logarithm.

As far as numerical integration is concerned, the Runge-Kutta-Fehlberg 4(5) scheme was used. Since it features step-size control, it required some adaptation for the algebras. In order to compute the estimated error, the central value was used for Taylor while the upper bound of the corresponding polynomial was used for Tchebycheff, estimated via its coefficients.

The uncertain state variables considered via the intrusive approach are the initial position and velocity of the object. The other uncertain parameters are related to drag. Describing the object itself, there are its mass, cross-sectional area and drag coefficient, assuming a spherical representation for its aerodynamic geometry. Only two uncertain parameters are not dependent of the object: the mean solar flux and the geomagnetic index. These quantities are parameters in the computation of atmospheric density. They are assumed to be constant over time for the duration of the simulation.

III.ii Propagation with Keplerian coordinates

This propagator simulates the effects of atmospheric drag on osculating orbital elements, assuming a spherical shape for aerodynamics. It is based on equations given in Bezdek and Vokrouhlicky[11] that are written with the eccentric anomaly as the independent variable. They provide state derivatives for long-term effects in the variation of semi-major axis a, eccentricity e, inclination i and argument of perigee ω (the variation of the right ascension of the ascending node being neglected). The model used here for atmospheric density is simply an exponential term, assuming a uniform scale factor over the whole range of altitudes. The Earth's oblateness is not taken into account.

The integration scheme is Runge-Kutta 4. The uncertain state variables are the Keplerian coordinates a, e, i and ω. Uncertainty on the aerodynamics is gathered in one single quantity $C_D A/m$ i.e. the product between the drag coefficient and the area-to-mass ratio. The last two uncertain parameters are the reference values used to define the uniform exponential scale of the atmospheric density, namely at altitudes 120 and 1000km.

IV. Results

This section will present the results obtained for two cases of study: the de-orbiting and re-entry of the GOCE mission of ESA and a more generic scenario concerning the de-orbiting of objects with high area-to-mass ratio.

IV.i De-orbiting and re-entry of GOCE

Three examples are presented hereby, simulating consecutive stages in GOCE's orbit decay. In late October and early November 2013, shortly before its re-entry, the ESA spacecraft was on a polar orbit with altitudes around 200km. Nominal values for initial position and velocity at initial epoch are taken from the Precise Orbit Determination performed over this period. Other nominal parameters of interest are summarised in Table 1.

Table 1: Nominal parameters, GOCE test cases.

Mass	1002.152 kg
1 Cross-sectional area	1.6286 m^2
Drag coefficient C_D	2.0
Mean solar flux	$132 \cdot 10^{-22}$ W/(m^2Hz)
Geomagnetic index	3.22

In all cases, the uncertain region has been propagated by means of the Tchebycheff approach proposed as well as using Taylor Differential Algebra. All uncertain quantities are thus represented by polynomials in 10 variables. Comparison between the two intrusive methods is provided in terms of accuracy and run-time. A uniform Monte Carlo sample of cardinality $N_s = 10^5$ of the initial uncertain region has been propagated and the results taken as reference values. Root mean square errors (RMSE) and peak errors in the radial, transverse and binormal directions ($\mathbf{r}$, $\mathbf{t}$ and $\mathbf{h}$, resp.) are reported, defined as

$$RMSE_x = \sqrt{\frac{1}{N_s}\sum_{i=1}^{N_s}(\hat{x}_i - x_i)^2}\ ,$$

$$max.\ err_x = \max_{1\le i\le n}\left(|\hat{x}_i - x_i|\right),$$

where x_i is the true value of the state obtained by forward integration of the sample and $\hat{x}_i$ is the approximate value computed evaluating the polynomial expansion obtained with one or the other algebra. Run-times have been scaled with the total CPU time required for the aforementioned direct propagation.

GOCE Example 1

The first simulation is initialised at 03:00:00 on 22/10/2013 and spans 8 days. The set up regarding uncertainties considered is summarised in Table 2.

The accuracy and run-time results for this example are reported in Table 3. It is interesting to remark that for this test case, an increase in the degree of the algebra is

Table 2: Uncertainties, GOCE example 1.

Initial positions (x, y, z)	$\pm$ 0.1 km
Initial velocities $(\dot{x}, \dot{y}, \dot{z})$	$\pm$ 0.1 m/s
Mass	$\pm$ 0.1 kg
Cross-sectional area	$\pm$ 0.4 m^2
Mean solar flux	$\pm$ 5 $\cdot$ 10^{-22} W/(m^{2}Hz)
Geomagnetic index	$\pm$ 0.6

not producing a notable improvement in terms of mean accuracy with either of the two methods tested. For the Tchebycheff approach, using a higher order appears to translate into a slight reduction of the maximum errors, the RMSE values remaining approximately constant. In the case of the Taylor differential algebra, both error measures increase with the order. In particular, at degree 5 the maximum error peaks and the expansions start to diverge in the distal sections of the uncertain region. This is due to numerical instability in relation to the high-order terms of the algebra, and it proves that stability issues, bound to occur for high orders and long simulation times, can be delayed with the use of Tchebycheff approximation. This is specially true for simulations such as this one, where some elements in the model are piece-wise-defined and do not present infinite differentiability between their subdomains; the Tchebycheff approximation method will smooth these non-differentiabilities as soon as they appear within the bounds of the domain, whereas Taylor algebra will only take them into account when the central point crosses from one subdomain to another, thus experiencing an abrupt change of state. Nevertheless, it is worth noticing that, Taylor differential algebra being a local approach, its accuracy in the vicinity of the central point is fairly good even in such a near-divergence situation, as can be observed in Figure 2. The Tchebycheff-based approach is not spared by numerical issues, even if they occur at higher orders than with Taylor. For this example, Tchebycheff expansions start to diverge at degree 6, leading to coefficients that are orders of magnitude higher than expected. No meaningful information can then be retrieved from the polynomials obtained, not even for the nominal set of parameters, which is also explained by the fact that this method attempts global approximation over an interval and, as a result, failure to converge is global as well.

GOCE Example 2

This simulation is initialised at 03:00:00 on 30/10/13 and covers 10 days of flight. With respect to Example 1, a larger uncertainty is considered in the initial velocity, whereas tighter bounds are set for the drag force pa-

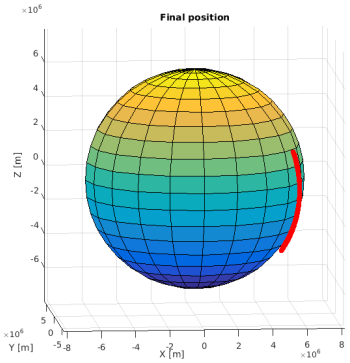

Fig. 1: Final position: Monte Carlo sample of 10^5 points, GOCE example 1.

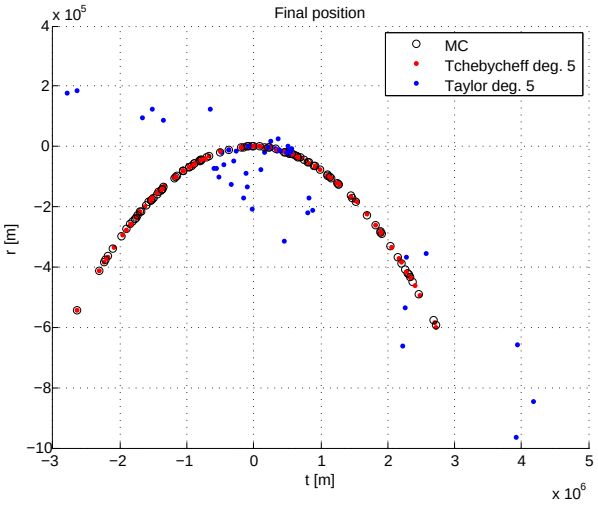

Fig. 2: Final position comparison between Tchebycheff and Taylor algebras of order 5 and Monte Carlo sample of 10^2 points, $< \mathbf{t}, \mathbf{r} >$ plane, GOCE example 1.

rameters. The uncertainty values considered are shown in Table 4.

The accuracy and run-time results for this example are reported in Table 5. By comparing Figures 4 and 1 one notices that the longer simulation time and the higher uncertainty on initial velocity lead to a much larger final uncertain region, spanning almost half a revolution. This is too large a domain to be represented accurately with a single set of polynomial expansions, which explains why both intrusive approaches give less accurate results than in the previous example. In order to evaluate this hypothesis, a non-intrusive approach based on Tchebycheff hyperinterpolation of the final states is applied on a subset of the Monte Carlo sample. The results, for degree 5, yield errors of the order of 50% of those of the intrusive; its ac-

Table 3: Errors and run-time, GOCE example 1. All errors in [km].

Approach	Order	RMSE_r	Max. err_r	RMSE_t	Max. err_t	RMSE_h	Max. err_h	Run-time
Taylor	3	3.242	26.432	13.207	68.231	0.007	0.049	0.027
Tchebycheff	3	3.256	26.951	13.156	74.859	0.007	0.050	0.037
Taylor	4	2.600	18.536	22.839	238.236	0.007	0.055	0.076
Tchebycheff	4	3.092	27.057	14.644	46.610	0.007	0.045	0.095
Taylor	5	$3.457{\cdot}10^3$	$4.309{\cdot}10^4$	$3.669{\cdot}10^4$	$5.347{\cdot}10^5$	8.773	124.341	0.281
Tchebycheff	5	3.014	26.064	12.320	47.187	0.006	0.023	0.326

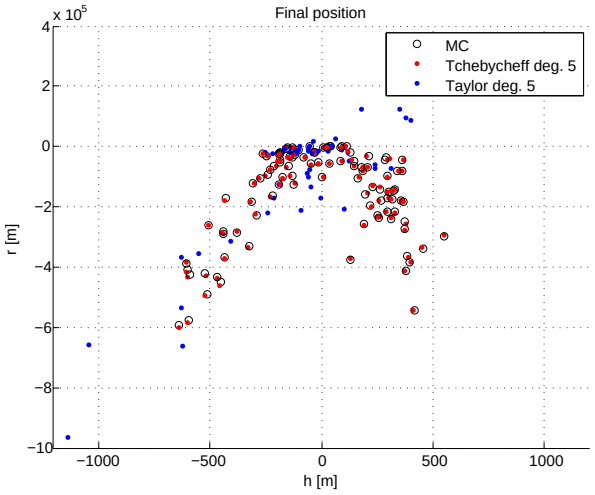

Fig. 3: Final position comparison between Tchebycheff and Taylor algebras of order 5 and Monte Carlo sample of 10^2 points, $< \mathbf{h}, \mathbf{r} >$ plane, GOCE example 1.

curacy, although better, can still be considered relatively poor, which confirms the difficulty in representation of the domain. The run-time of the non-intrusive technique is also much shorter in this case (0.032 in scaled unit), due to the fact that intrusive methods become advantageous in terms of computational performance only with a larger number of uncertain parameters for a simulation of this complexity.

Figures 5 and 6 show a comparison between a subset of cardinality 10^2 of the Monte Carlo sample and the evaluation in the same subset of the final Tchebycheff and Taylor expansions of order 4. Once again the local nature of the Taylor approach is manifest, yielding acceptable representation of the vicinity of the central point even in near-divergence. Note that the polynomial approximations obtained with the Tchebycheff algebra also show lower accuracy in the distal sections of the uncertain region, but in a much more subtle fashion. This is due to the fact that numerical error in the coefficients of the polynomials will

Table 4: Uncertainties, GOCE example 2.

Initial positions (x, y, z)	$\pm$ 0.1 km
Initial velocities $(\dot{x}, \dot{y}, \dot{z})$	$\pm$ 1.0 m/s
Mass	$\pm$ 0.1 kg
Cross-sectional area	$\pm$ 0.2 m^2
Mean solar flux	$\pm$ 2.5 $\cdot$ 10^{-22} W/(m^2Hz)
Geomagnetic index	$\pm$ 0.3

have a larger impact in the edges of the uncertain set of parameters, where the high-order terms are relevant, thus its effect has a smaller impact than the effect of a local approximation technique. As regards the trend of the error with the degree, the intrusive methods behave in a similar way to example 1, with the difference that the drop in accuracy in the Taylor algebra appears at degree 4 instead of 5. The Tchebycheff approach is also diverging at order 6.

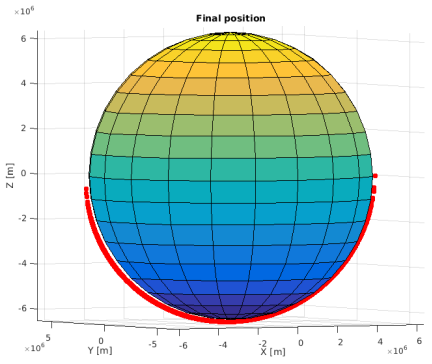

Fig. 4: Final position: Monte Carlo sample of 10^5 points, GOCE example 2.

GOCE Example 3

This simulation is initialised at 03:00:00 on 09/11/2013 and spans 31 hours, covering the final stage of the deorbiting process. The uncertainties considered are the largest among the three examples presented, as shown in Table 6.

Table 5: Errors and run-time, GOCE example 2. All errors in [km].

Approach	Order	RMSE_r	Max. err_r	RMSE_t	Max. err_t	RMSE_h	Max. err_h	Run-time
Taylor	3	122.613	$1.657{\cdot}10^3$	151.695	$1.625{\cdot}10^3$	0.184	2.640	0.027
Tchebycheff	3	120.529	$1.525{\cdot}10^3$	126.876	$1.333{\cdot}10^3$	0.181	2.587	0.049
Taylor	4	$1.174{\cdot}10^3$	$1.200{\cdot}10^4$	$1.535{\cdot}10^4$	$1.680{\cdot}10^5$	20.353	218.861	0.071
Tchebycheff	4	87.039	$1.129{\cdot}10^3$	66.847	289.450	0.118	1.762	0.126
Tchebycheff	5	88.749	$1.057{\cdot}10^3$	91.609	301.194	0.078	0.383	0.367

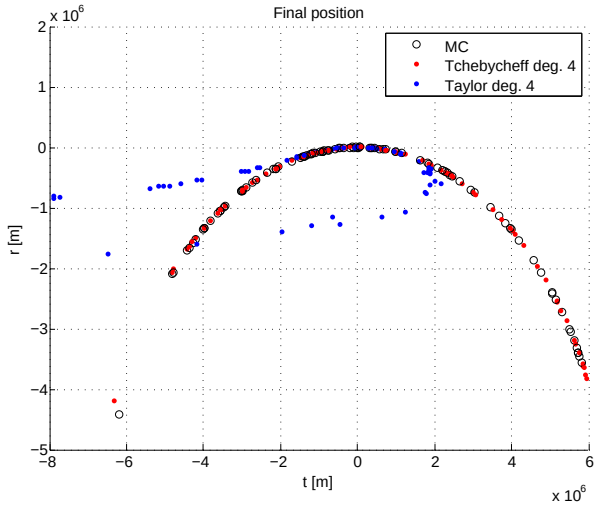

Fig. 5: Final position comparison between Tchebycheff and Taylor algebras of order 4 and Monte Carlo sample of 10^2 points, $< \mathbf{t}, \mathbf{r} >$ plane, GOCE example 2.

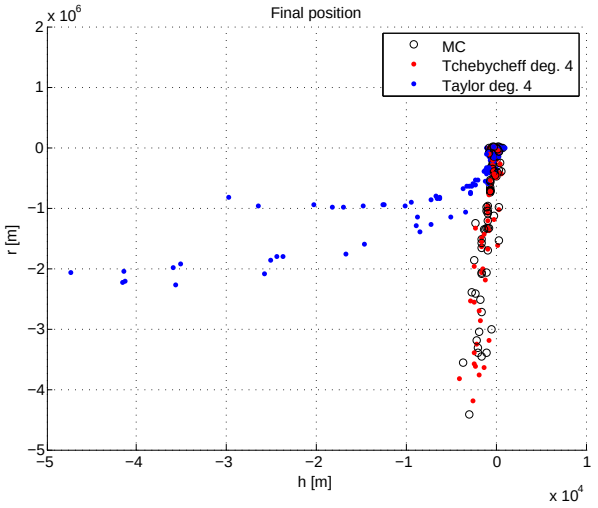

Fig. 6: Final position comparison between Tchebycheff and Taylor algebras of order 4 and Monte Carlo sample of 10^2 points, $< \mathbf{h}, \mathbf{r} >$ plane, GOCE example 2.

Results in Table 7 demonstrate the same trends discussed in the cases above. In particular, the Taylor approach loses accuracy in the $\mathbf{t}$ direction at degree 5, as shown in Figure 8. Note that, unlike in the previous examples, the Tchebycheff algebra of order 6 achieves convergence. This can be explained by the shorter simulation time span. Indeed, a longer propagation time yields a higher number of integration steps and thus a higher number of operations between polynomials, which leads to a growth in truncation error. The run-time of the Tchebycheff algebra of order 6 is larger than the propagation of the Monte Carlo sample of cardinality 10^5, but would still be one order of magnitude faster than the sampling of 10^6 occurrences.

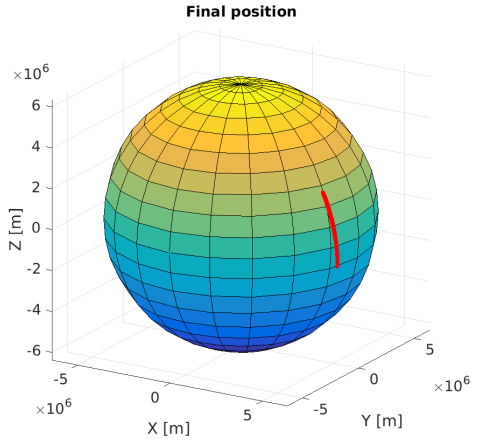

Fig. 7: Final position: Monte Carlo sample of 10^5 points, GOCE example 3.

IV.ii De-orbiting of objects with high area-to-mass ratio (HAMR)

The following examples simulate the orbital decay of a cloud of debris, as could result from an orbital collision. The focus is on objects with high area-to-mass ratios, e.g. pieces of solar panels or blankets. The intrusive approach allows for uncertainty on the initial spreading as well as

Table 6: Uncertainties, GOCE example 3.

Initial positions (x, y, z)	$\pm$ 1.0 km
Initial velocities $(\dot{x}, \dot{y}, \dot{z})$	$\pm$ 1.0 m/s
Mass	$\pm$ 0.1 kg
Cross-sectional area	$\pm$ 0.4 m^2
Mean solar flux	$\pm$ 5.0 $\cdot$ 10^{-22} W/(m^{2}Hz)
Geomagnetic index	$\pm$ 0.6

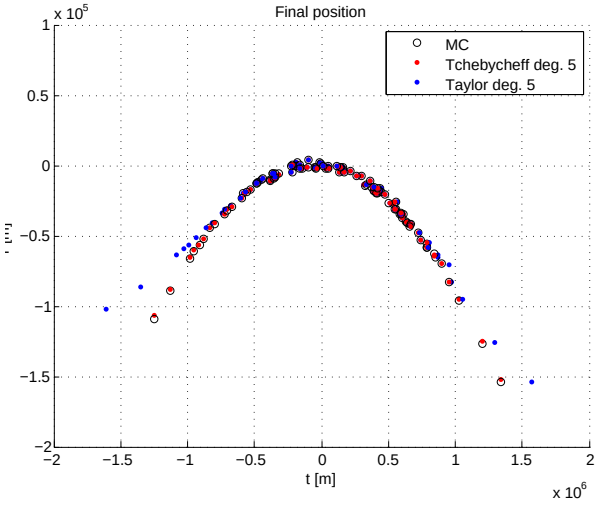

Fig. 8: Final position comparison between Tchebycheff and Taylor algebras of order 5 and Monte Carlo sample of 10^2 points, $< \mathbf{t}, \mathbf{r} >$ plane, GOCE example 3.

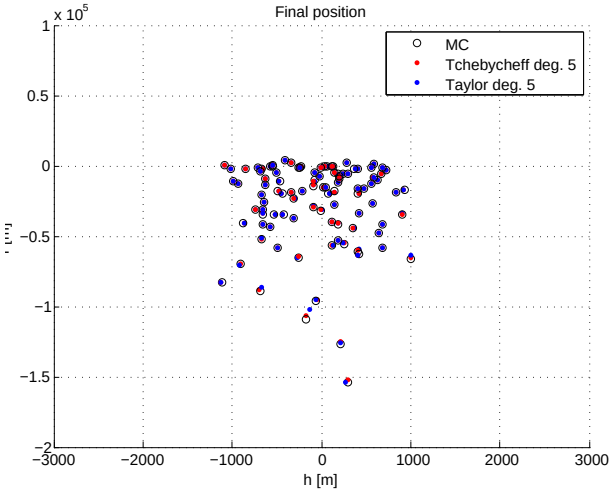

Fig. 9: Final position comparison between Tchebycheff and Taylor algebras of order 5 and Monte Carlo sample of 10^2 points, $< \mathbf{h}, \mathbf{r} >$ plane, GOCE example 3.

in the size of the pieces of satellites.

The interest of intrusive uncertainty propagation techniques for the study of debris lies in the possibility to propagate a cluster of objects at once, providing a time-wise polynomial representation of the evolution of this cluster. The availability of such a representation allows a great flexibility in analysis. Furthermore, this analysis can be conducted dynamically and used to enhance the simulations. Targeting a cloud of objects with high area-to-mass ratio in LEO will put to the test the extent to which such methods can capture the non-linearities inherent to the dynamics of orbital decay and deal with uncertain regions that evolve in an asymmetric fashion.

First a simplified analysis of the problem, considering only the long-term effects of drag, will be conducted by means of a propagation in the osculating orbital elements. Uncertainty is considered in the initial elements as well as in the parameters of the drag model, which is defined by the inverse of the ballistic coefficient, $\delta = C_D A/m$, and a uniform exponential model with reference densities ρ_0 and ρ_t specified at two reference altitudes, here 120 and 1000 km, respectively. The numerical set up is summarised in Table 8. A seven-dimensional polynomial algebra of order 4 is used for the propagation. Accuracy along the simulation is measured for both Taylor DA and Tchebycheff algebra.

In the remaining subsections, the same model as in IV.1 will be applied to the study of clusters of HAMR objects. Two examples are shown, labeled HAMR case 1 and 2, involving nominal area-to-mass ratios 4 and 3 orders of magnitude higher than that of GOCE, respectively. The propagation has been stopped when approaching the lower altitude limit of the atmospheric model used. Hence case 1 needs to be stopped much before case 2 since the cloud decays faster due to its higher area-to-mass ratios.

These two cases consider a nominal initial state defined by an orbit of 6800 km of semi-major axis and 30º of inclination, with the rest of orbital parameters set to zero. The common set up regarding nominal parameters and uncertainties are shown in Tables 9 and 10. Considering uncertainty also in the drag coefficient, simulations in the Taylor and Tchebycheff algebras operate with polynomials in 11 variables.

The format in which the results are presented for HAMR case 1 and 2 is identical to that of section IV.1.

HAMR in Keplerian coordinates

Figure 10 shows how the uncertainties affect the orbital decay and compares the ability of Taylor DA and Tchebycheff algebra to capture these dynamics. The effects of drag on the inclination are very small up to fifty revolutions and hence are not shown. The differences between the two algebras are barely perceptible, whereas it is pos-

Table 7: Errors and run-time, GOCE example 3. All errors in [km].

Approach	Order	RMSE_r	Max. err_r	RMSE_t	Max. err_t	RMSE_h	Max. err_h	Run-time
Taylor	3	3.211	105.579	4.716	146.813	0.005	0.215	0.024
Tchebycheff	3	3.215	105.656	4.678	144.956	0.005	0.215	0.054
Taylor	4	1.517	71.298	3.032	105.059	0.004	0.187	0.066
Tchebycheff	4	1.496	70.673	2.904	101.213	0.004	0.186	0.112
Taylor	5	0.793	45.836	41.429	911.541	0.005	0.103	0.249
Tchebycheff	5	0.832	51.900	2.463	76.222	0.004	0.165	0.322
Tchebycheff	6	0.530	40.039	2.313	58.638	0.004	0.149	1.222

Table 8: Nominal parameters and uncertainties, HAMR in Keplerian coordinates.

a	7500 ± 10 km
e	0.100 ± 0.005
i	$30 \pm 1^{\text{o}}$
ω	$180 \pm 1^{\text{o}}$
δ	0.22 ± 0.01
ρ_0	$2.438{\cdot}10^{-8} \pm 1.219{\cdot}10^{-9}$ kg/m^3
ρ_t	$3.019{\cdot}10^{-15} \pm 1.510{\cdot}10^{-16}$ kg/m^3

Table 9: Nominal parameters, HAMR test cases.

Mass	1.0 kg
Drag coefficient C_D	2.0
Mean solar flux	$150 \cdot 10^{-22}$ W/(m^{2}Hz)
Geomagnetic index	3.0

sible to remark that the errors with respect to the direct propagation increase with the length of the simulation, as shown in Tables 11 and 12, which report the evolution with the number of revolutions of the error measures obtained comparing Tchebycheff and Taylor algebra, respectively, with the direct propagation of a sample of cardinality 10^4.

For a point in the uncertain space, these results show the typical trend of orbital decay in elliptic orbits. Regarding the propagation of the uncertain set as a whole, note that the uncertain region can become very large as the simulation advances and some points in the set start re-entering. Due to the fast dynamics of re-entry, this will lead to a highly non-linear region that is increasingly difficult to capture with a single polynomial expansion.

HAMR case 1

This case considers a nominal area-to-mass ratio of 10 m^2/kg with uncertainty of $\pm 10\%$ and has been propagated for 4h 26min 24s.

Table 10: Uncertainties, HAMR test cases.

Initial positions (x, y, z)	$\pm$ 0.01 km
Initial velocities $(\dot{x}, \dot{y}, \dot{z})$	$\pm$ 0.1 m/s
Mass	$\pm$ 0.01 kg
Drag coefficient C_D	$\pm$ 0.2
Mean solar flux	$\pm\ 5 \cdot 10^{-22}$ W/(m^{2}Hz)
Geomagnetic index	$\pm$ 0.66

Table 11: Error measures along the simulation for altitudes of apogee (ap) and perigee (pe), Tchebycheff algebra of order 4, HAMR in Keplerian coordinates. All errors in [km].

Rev.	RMSE_{ap}	Max. err_{ap}	RMSE_{pe}	Max. err_{pe}
10	0.009	0.030	0.480	1.639
20	0.020	0.078	0.985	3.641
30	0.033	0.150	1.526	6.293
40	0.049	0.246	2.118	10.155
50	0.069	0.358	2.801	16.408

Results for accuracy and run-time are presented in Table 13. Due to the very short simulation time and small uncertain region, all errors are moderate and there is no divergence of any of the methods up to degree 6. For the same reason, there are no remarkable differences between the errors attained by the Tchebycheff and Taylor Algebras. Figures 11 and 12 show the asymmetric final uncertain region obtained by the direct simulation and the intrusive techniques of order 5, the minimum altitude attained by the former being around 100km. Note that due to the large impact of drag on the dynamics, the uncertain region spans out of the osculating plane in a more abrupt fashion than in IV.1.

HAMR case 2

This case considers a nominal area-to-mass ratio of 1 m^2/kg with uncertainty of $\pm 10\%$ and has been propagated

Table 12: Error measures along the simulation for altitudes of apogee (ap) and perigee (pe), Taylor algebra of order 4, HAMR in Keplerian coordinates. All errors in [km].

Rev.	RMSE$_{ap}$	Max. err$_{ap}$	RMSE$_{pe}$	Max. err$_{pe}$
10	0.009	0.030	0.480	1.640
20	0.020	0.078	0.985	3.647
30	0.033	0.149	1.526	6.310
40	0.049	0.245	2.118	10.195
50	0.069	0.354	2.802	16.491

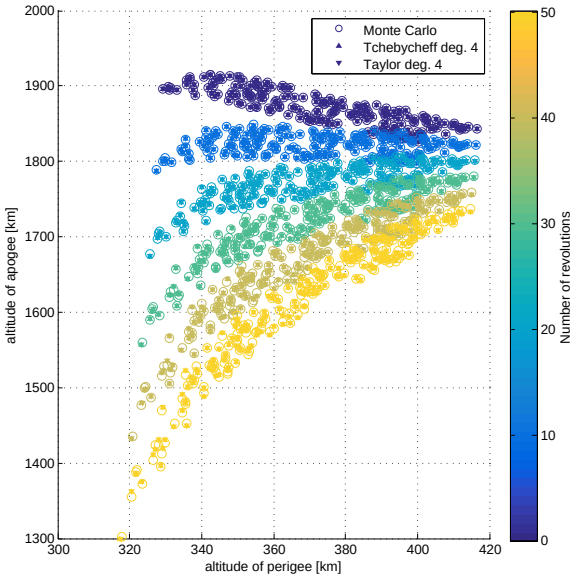

Fig. 10: Altitudes of apogee vs. altitudes of perigee for HAMR in Keplerian coordinates in several stages of the uncertainty propagation.

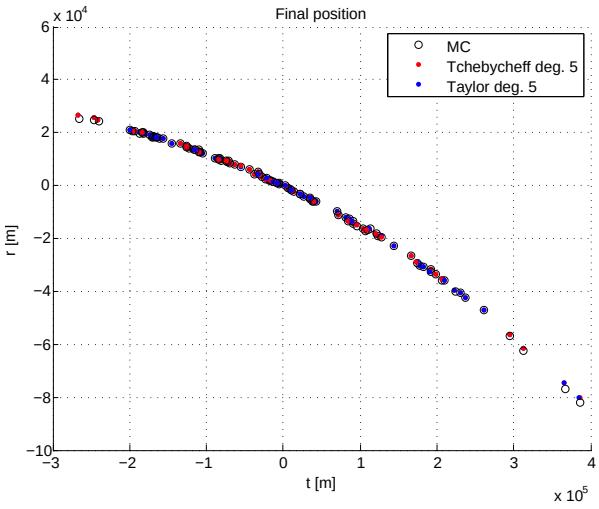

Fig. 11: Final position comparison between Tchebycheff and Taylor algebras of order 5 and Monte Carlo sample of 10^2 points, $< \mathbf{t}, \mathbf{r} >$ plane, HAMR case 1.

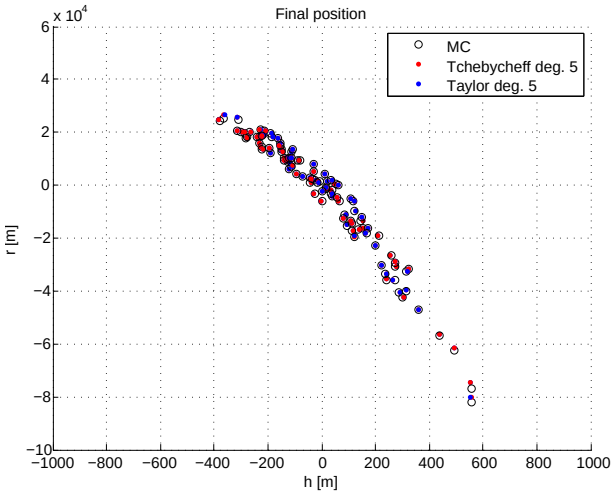

Fig. 12: Final position comparison between Tchebycheff and Taylor algebras of order 5 and Monte Carlo sample of 10^2 points, $< \mathbf{h}, \mathbf{r} >$ plane, HAMR case 1.

for 1day 14h 24min.

Results for accuracy and run-time are presented in Table 14. Figures 13 and 14 show the final uncertain region in terms of position. Note that the asymmetry is clear but not as extreme as in case 1 since the propagation has been stopped at a higher minimum altitude.

The error measures obtained are overall still good but larger than in case 1, with RMSE values around one order of magnitude higher in the $\mathbf{r}$ and $\mathbf{t}$ directions. This is so because, even if the initial uncertainties are significantly smaller and the asymmetry less extreme, the simulation time is one order of magnitude larger, and hence the numerical and truncation error that accumulates along the propagation is manifest. As has been argued in IV.1, it is this same effect that causes Taylor DA to follow a different trend from Tchebycheff, presenting loss or no significant gain of accuracy from degree 4 to 5, and divergence at degree 6.

V. Conclusions

The paper presents a Generalised Intrusive Polynomial Expansion (GIPE) approach to propagate generic sets through dynamical systems and illustrates its application to end-of-life analysis of Low Earth Orbit objects.

Table 13: Errors and run-time, HAMR case 1. All errors in [km].

Approach	Order	RMSE_r	Max. err_r	RMSE_t	Max. err_t	RMSE_h	Max. err_h	Run-time
Taylor	3	2.937	112.406	2.395	61.711	0.011	2.742	0.025
Tchebycheff	3	2.983	113.388	2.442	61.011	0.011	2.737	0.033
Taylor	4	1.761	86.684	1.069	89.749	0.011	2.817	0.079
Tchebycheff	4	1.779	86.984	1.069	90.138	0.011	2.817	0.098
Taylor	5	1.172	69.399	0.679	102.889	0.011	2.852	0.341
Tchebycheff	5	1.133	67.911	0.638	105.428	0.011	2.861	0.410
Taylor	6	0.861	57.725	0.607	108.401	0.011	2.863	1.420
Tchebycheff	6	0.809	55.598	0.583	111.329	0.011	2.870	1.759

Table 14: Errors and run-time, HAMR case 2. All errors in [km].

Approach	Order	RMSE_r	Max. err_r	RMSE_t	Max. err_t	RMSE_h	Max. err_h	Run-time
Taylor	3	21.820	564.628	8.277	181.444	0.042	1.229	0.024
Tchebycheff	3	21.784	564.164	8.089	179.452	0.042	1.230	0.032
Taylor	4	10.638	365.054	6.285	145.775	0.021	0.832	0.079
Tchebycheff	4	10.647	365.108	6.269	144.819	0.022	0.834	0.095
Taylor	5	8.196	313.276	8.713	185.892	0.018	0.777	0.349
Tchebycheff	5	6.610	268.453	5.697	132.896	0.012	0.589	0.404
Taylor	6	$3.641{\cdot}10^3$	$1.018{\cdot}10^5$	$6.277{\cdot}10^4$	$1.759{\cdot}10^6$	32.534	913.46	
Tchebycheff	6	4.767	214.34	5.450	123.688	0.008	0.448	

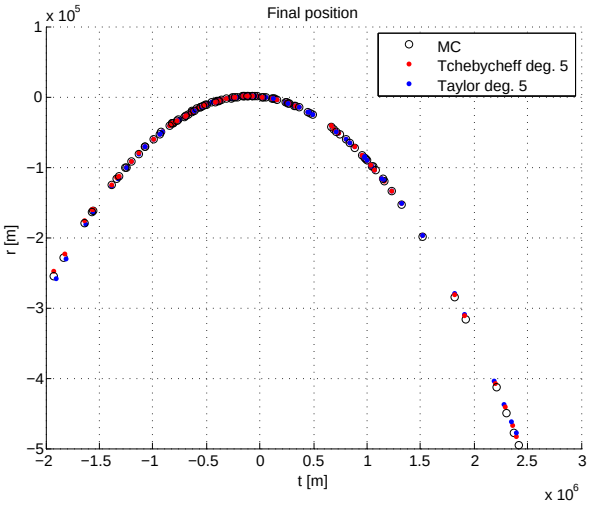

Fig. 13: Final position comparison between Tchebycheff and Taylor algebras of order 5 and Monte Carlo sample of 10^2 points, $< \mathbf{t}, \mathbf{r} >$ plane, HAMR case 2.

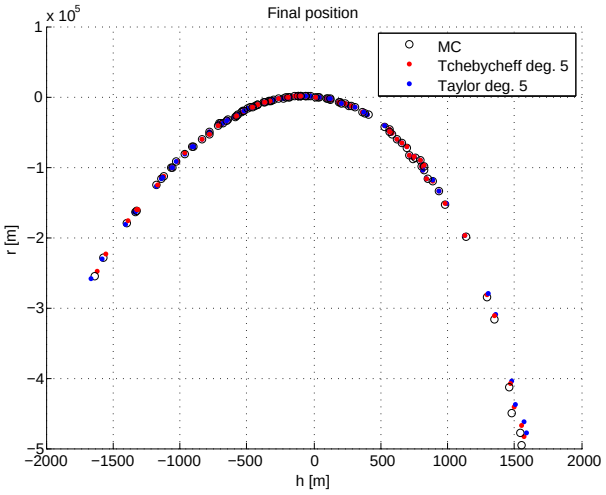

Fig. 14: Final position comparison between Tchebycheff and Taylor algebras of order 5 and Monte Carlo sample of 10^2 points, $< \mathbf{h}, \mathbf{r} >$ plane, HAMR case 2.

In particular, it can be used to study the evolution of pieces of satellites with high area-to-mass ratios resulting from a collision in LEO.

Intrusive uncertainty propagation methods present several implementation drawbacks with respect to their non-intrusive counterparts. Namely, they require a modification of the deterministic simulation solver and will need a larger number of operations for a single step of simu-

lation. On the other hand, they remove the necessity to propagate a sample and train a surrogate model, since the model itself is propagated through the simulation. This is a very powerful feature by itself; the model being available at any time, dynamic analysis is made possible. Furthermore, it translates into a much lower computational complexity when the number of uncertain parameters is high enough and/or the simulation dynamics are simple enough. Problems with these properties are relatively common in astrodynamics.

In the GIPE modular framework the propagation is conducted by means of a polynomial algebra in the monomial basis that relies on an arbitrary function approximation method, and can hence be set to act as a differential algebra or as a hyperinterpolation-based algebra. This versatility has been taken advantage of to provide a comparison between Taylor Differential Algebra and Tchebycheff Algebra that is representative of the general properties of these two families of polynomial algebras.

The key difference between differential and hyperinterpolation-based approaches is that the former use local derivative-based function approximation methods in the vicinity of the nominal set of parameters, referred to as central point, while the latter rely on hyperinterpolation techniques that attempt global convergence over an interval whose bounds are estimated. The practical implications of this are that, whereas differential algebras are more robust for dynamics presenting inherent singularities that cannot be avoided by reformulation (e.g. simulation of a gravity assist), interval-based approaches are less prone to experience numerical instability when dealing with discontinuities and non-differentiabilities in the simulation model (e.g. with piecewise-defined empirical models, as most atmospheric models are). The results discussed hereby, which make use of the Jacchia-Gill atmospheric model, prove that one can delay the apparition of such instabilities with very slight loss in computational performance, by using a hyperinterpolation-based method such as the proposed Tchebycheff Algebra. This is especially so when dealing with uncertain regions that are large with respect to the characteristic units of the simulation. On the other hand, when these instabilities appear they will provoke global failure to represent the uncertain region, whereas with Taylor Differential Algebra one can obtain relatively acceptable accuracy near the central point even in near-divergence situations.

REFERENCES

[1] M. Berz. The new method of TPSA algebra for the description of beam dynamics to high orders. Tech. Report AT–6: TN–86–16, Los Alamos National Laboratory, Los Alamos, N.M., 1986.

[2] M. Berz. The method of power series tracking for the mathematical description of beam dynamics. *Nuclear Instruments and Methods*, A258:431 +, 1987.

[3] P. Di Lizia, R. Armellin, and M. Lavagna. Application of high order expansions of two-point boundary value problems to astrodynamics. *Celestial Mechanics and Dynamical Astronomy*, 102(4):355–375, 2008.

[4] R. Armellin, P. Di Lizia, F. Bernelli-Zazzera, and M. Berz. Asteroid close encounters characterization using differential algebra: the case of apophis. *Celestial Mechanics and Dynamical Astronomy*, 107 (4):451–470, 2010.

[5] P. Di Lizia, R. Armellin, A. Morselli, and F. Bernelli-Zazzera. High order optimal feedback control of space trajectories with bounded control. *Acta Astronautica*, 94(1):383–394, 2014.

[6] A. Jorba and M. Zou. A software package for the numerical integration of odes by means of high-order taylor methods. *Experimental Mathematics*, 14, 2005.

[7] N. Brisebarre and M. Joldes. Chebyshev interpolation polynomial-based tools for rigorous computing. In *Proceedings of the 2010 International Symposium on Symbolic and Algebraic Computation*, ISSAC '10, pages 147–154. ACM, New York, NY, USA, 2010. ISBN 978-1-4503-0150-3.

[8] A. Riccardi and M. Vasile C. Tardioli. An intrusive approach to uncertainty propagation in orbital mechanics based on tchebycheff polynomial algebra. In *Proceedings of the AAS/AIAA Astrodynamics Specialist Conference*. Vail, Colorado, August 2015.

[9] C. Ortega, A. Riccardi, M. Vasile, and C. Tardioli. Smart-uq: Uncertainty quantification toolbox for generalised intrusive and non-intrusive polynomial algebra. In *6th International Conference on Astrodynamics Tools and Techniques*, 2016.

[10] Oliver Montenbruck and Eberhard Gill. *Satellite orbits: models, methods and applications*. Springer Science & Business Media, 2012.

[11] A Bezděk and D Vokrouhlickỳ. Semianalytic theory of motion for close-earth spherical satellites including drag and gravitational perturbations. *Planetary and Space Science*, 52(14):1233–1249, 2004.